

## ISOTOPIC EVIDENCE FOR VOLATILE REPLENISHMENT OF THE MOON DURING LATE ACCRETION.

Yanhao Lin\* and Wim van Westrenen, Department of Earth Sciences, Faculty of Science, Vrije Universiteit Amsterdam, The Netherlands (y.lin@vu.nl)

**Introduction:** The abundance and isotopic composition of hydrogen and chlorine in apatite provide one of a limited set of windows into the origin and history of the volatile budget of the Moon. Many studies have reported high-precision apatite volatile abundance (H, Cl, F) and isotopic measurements (D/H,  $\delta^{37}\text{Cl}$ ) from both lunar meteorites [1,2] and Apollo samples [2-14]. Typically these studies focus on identifying and explaining variations among and between distinct petrological groups (e.g., low-titanium and high-titanium mare basalts, KREEP (enriched in potassium (K), rare earth elements (REE) and phosphorus (P)) basalts, and highland samples), in terms of igneous processes including fractional crystallization, degassing, and mixing. Here, we present a compilation of measurements performed to date, and show unexpected variations in apatite isotopic values as a function of the age of the rocks in which the apatites formed. These variations are used to provide new constraints on the lunar interior volatile cycle.

**Database:** We have compiled all lunar apatite volatile abundance and isotopic measurements published over the past ~10 years. For most samples, either hydrogen or chlorine isotopes were measured. Deuterium/hydrogen (D/H) ratios are reported using  $\delta\text{D}$  values, with  $\delta\text{D} = \left\{ \left[ \frac{(\text{D}/\text{H})_{\text{sample}}}{(\text{D}/\text{H})_{\text{VSMOW}}} - 1 \right] \times 1,000 \right\}$  (VSMOW: Vienna standard mean ocean water).  $^{37}\text{Cl}/^{35}\text{Cl}$  ratios, reported using  $\delta^{37}\text{Cl}$  values, with  $\delta^{37}\text{Cl} = \left\{ \left[ \frac{(^{37}\text{Cl}/^{35}\text{Cl})_{\text{sample}}}{(^{37}\text{Cl}/^{35}\text{Cl})_{\text{SMOC}}} - 1 \right] \times 1,000 \right\}$  (SMOC: standard mean ocean chloride). We have also collected measured ages for the samples in which the apatites were found. Sample ages are predominantly whole rock ages, and we assume that these are representative for the ages of the apatites themselves. Figures 1 and 2 show our resulting data set for H and Cl, respectively.

**Results and Discussion:** Plotting all individual measured isotopic compositions of samples as a function of their inferred age (Figs. 1B and 2B) reveals previously undetected and striking changes in apatite isotopic composition through time, centered around the second stage of the Late Heavy Bombardment at ~4.1–3.8 Ga (termed Late Accretion, LA) [15,16].

As discussed by previous studies [13], the absence of a negative correlation between OH abundances in apatite and their  $\delta\text{D}$  (Fig. 1A) shows that degassing is not the source of the trend seen in Fig. 1A. Late-stage degassing is also inconsistent with Cl isotopic data (Fig. 2B).

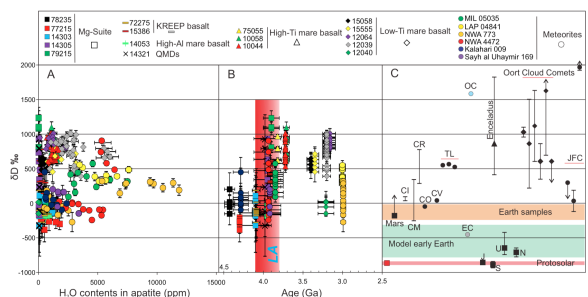


Figure 1. Compilation of hydrogen isotopic composition, water content and crystallization ages in lunar apatite ( $n = 260$ , mention number of analyses shown). D/H ratios are shown versus measured OH abundances in ppm (A) and versus sample crystallization age (B). LA = Late Accretion. Panel (C) shows the hydrogen isotopic composition of major solar system reservoirs including Earth; Mars, Jupiter (J), Saturn (S), Uranus (U) and Neptune (N); Saturn's Moon Enceladus; chondrite groups carbonaceous chondrites groups CI, CM, CR, CO and CV; Tagish Lake samples 11i, 11h and 5b (TL); Oort Cloud Comets 1P/Halley, Hyakutake, Hale-Bopp, C/2002 T7 (LINEAR), 8P Tuttle and 153P/Ikeya-Zhang, respectively; and JFC, Jupiter-family comet. Arrows indicate  $\delta\text{D}$  values beyond the maximum or minimum of the Y axis scale. Error bars are  $2\sigma$ .

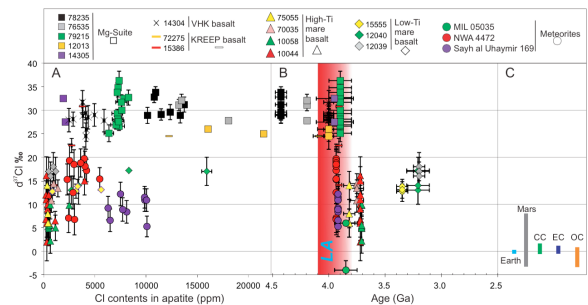


Figure 2. Compilation of chlorine isotopic composition, chlorine content and crystallization ages in lunar apatite ( $n = 90$ , mention number of analyses shown).  $^{37}\text{Cl}/^{35}\text{Cl}$  ratios are shown versus measured Cl abundances in ppm (A) and versus sample crystallization age (B). LA = Late Accretion. Panel (C) shows the chlorine isotopic composition of major solar system reservoirs including Earth; average of carbonaceous chondrite groups CI, CM, CR, CO, and CV (CC); enstatite chondrites (EC) and ordinary chondrites (OC). Error bars are  $2\sigma$ .

Alternatively, the  $\delta\text{D}$  increase and  $\delta^{37}\text{Cl}$  decrease can be explained by the addition of deuterium-rich and lighter Cl isotopic material to the Moon during LA. Addition of ordinary chondrites (OC) could lead to an increase and decrease in  $\delta\text{D}$  (Fig. 1C) and  $\delta^{37}\text{Cl}$  (Fig. 2C), respectively, from pre-LA to post-LA values, with

the large variability during LA reflecting variable mixing between the indigenous and added reservoirs.

Combined, Figs. 1 and 2 thus provide isotopic evidence for the addition of OC material to the Moon during late accretion. The fact that this OC component is measurable in volcanic samples implies LA impactors were capable of breaching the primitive lunar crust and mixing (albeit certainly not perfectly) with the lunar mantle source of the volcanics, consistent with the Barnes et al. model [4].

The H<sub>2</sub>O and Cl concentrations in apatite shown in Figs. 1 and 2 can be used to quantify lunar interior H<sub>2</sub>O and Cl contents. Quantification requires assumptions about (1) the partitioning of H<sub>2</sub>O and Cl between apatite and melt (2) a mantle melting model leading to the crystallization of apatite. Quantifying apatite-melt partitioning of volatiles is not straightforward [17]. The apatite-melt volatile exchange coefficient K<sub>d</sub> for OH-Cl is constant at 0.06±0.02 [17]. This exchange coefficient can be used to estimate quantitatively the water content of the mantle source if Cl contents in apatite and the corresponding parent melt are known [17]. We derived the Cl content of parent melt by combining measured lunar whole-rock Nd and Ba contents with the constant Cl/Nd and Cl/Ba ratios observed in primitive lunar magmatic samples [18]. Parent melts were estimated to have formed by partially melting a mantle source to a melt fraction of 15 per cent. As a result, the abundances of water in their mantle source are estimated to be ~1 ppm for pre-LA and ~33 ppm for post-LA by the Nd-based calculations. This suggests an increase from pre-LA source rock water contents of ~1 ppm to post-LA source rock water contents of ~33 ppm based on Cl/Nd. Cl/Ba-based calculations indicate ~3 ppm water in the lunar interior pre-LA versus ~45 ppm water post-LA, consistent with the Nd-based estimates.

Experiments simulating the solidification of the lunar magma ocean in the presence of water suggest the Moon contained at least 270 ppm water during the crystallization of its magma ocean [19], i.e. before any of the apatites considered in our compilation formed. Our compilation suggests that by the time the oldest apatites shown in Figures 1 and 2 formed, the lunar interior only contained ~1-3 ppm water, pointing to significant degassing of the Moon in the period before the formation of the apatites in the current database. The increase in water content from ~1-3 ppm pre-LA to 33-45 ppm post-LA again suggests that significant amounts of volatiles were added to the Moon during LA.

**Conclusions:** Our analysis indicates that the lunar interior volatile cycle is not characterized solely by progressive volatile loss from an initially volatile-rich

body. Our analysis suggests that the initially substantial water content of the Moon decreased significantly between the time of its formation and the start of late accretion, after which increases in D/H ratio and lowering of Cl isotopic composition occurred, accompanied by an increase in water content. This suggests that the Moon's (and by extension the Earth's) initial volatiles were replenished ~0.5 Ga after their formation, with final budgets reflecting a mixture of sources and delivery times. These findings are consistent with dynamic models that predict influxes of chemically and isotopically distinct asteroid populations at different times during the first ~700 million years of solar system evolution [20-23].

#### References:

- [1] Boyce J. W. et al. (2015) *Sci. Adv.* 1, 1-8.
- [2] Tartèse R. et al. (2013) *Geochim. Cosmochim. Acta* 122, 58-74.
- [3] Barnes J. J. et al. (2014) *Earth Planet. Sci. Lett.* 390, 244-252.
- [4] Barnes J. J. et al. (2016a) *Earth Planet. Sci. Lett.* 447, 84-94.
- [5] Barnes J. J. et al. (2016b) *Nat. Comm.* 7, 11684.
- [6] Boyce J. W. et al. (2010) *Nature*, 466, 466-469.
- [7] Tartèse R. and Anand M. (2013) *Earth Planet. Sci. Lett.* 361, 480-486.
- [8] Tartèse R. (2014a) *Geology*, 42, 363-366.
- [9] McCubbin F. M. et al. (2010a) *Am. Mineral.* 95, 1141-1150.
- [10] McCubbin F. M. (2010b) *Proc. Natl. Acad. Sci. USA*, 107, 11223-11228.
- [11] McCubbin F. M. et al. (2015a) *Am. Mineral.* 100, 1668-1707.
- [12] Sharp Z. D. et al. (2010) *Science*, 329, 1050-1053.
- [13] Greenwood J. P. et al. (2011) *Nat. Geosci.* 4, 79-82.
- [14] Robinson K. L. et al. (2016) *Geochim. Cosmochim. Acta* 188, 244-260.
- [15] Bottke W. F. and Norman M. D. (2017) *Annu. Rev. Earth Planet. Sci.* 45(1), 619-647.
- [16] Morbidelli A. and Wood B. J. (2015) *The Early Earth: Accretion and Differentiation* 71-82.
- [17] McCubbin F. M. (2015b) *Am. Mineral.* 100, 1790-1802.
- [18] Hauri E. H. (2015) *Earth Planet. Sci. Lett.* 409, 252-264.
- [19] Lin Y. (2017) *Nat. Geosci.* 10, 14-18.
- [20] Morbidelli A. (2000) *Meteor. & Planet. Sci.* 35, 1309-1320.
- [21] Bouvier A. and Wadhwa M. (2010) *Nat. Geosci.* 3, 637-641.
- [22] Walsh K. J. et al. (2011) *Nature*, 475, 206-209.
- [23] Walsh K. J. et al. (2012) *Meteor. & Planet. Sci.* 47, 1941-1947.